nature climate change

ARTICLES

https://doi.org/10.1038/s41558-021-01216-1

Health co-benefits of climate change mitigation depend on strategic power plant retirements and pollution controls

Dan Tong[1,2,5], Guannan Geng[3,5], Qiang Zhang[1]✉, Jing Cheng[1], Xinying Qin[1], Chaopeng Hong[2], Kebin He[3,4] and Steven J. Davis[2]✉

Reducing CO_2 emissions from fossil fuel- and biomass-fired power plants often also reduces air pollution, benefitting both climate and public health. Here, we examine the relationship of climate and health benefits by modelling individual electricity-generating units worldwide across a range of climate–energy policy scenarios. We estimate that ~92% of deaths related to power plant emissions during 2010–2018 occurred in low-income or emerging economies such as China, India and countries in Southeast Asia, and show that such deaths are quite sensitive to future climate–energy trajectories. Yet, minimizing future deaths will also require strategic retirements of super-polluting power plants and deployment of pollution control technologies. These findings underscore the importance of considering public health in designing and implementing climate–energy policies: improved air quality and avoided air pollution deaths are not an automatic and fixed co-benefit of climate mitigation.

Globally, electricity generation accounts for about one-seventh of humans' exposure to harmful air pollutants such as fine particulate matter with an aerodynamic diameter of 2.5 μm or less ($PM_{2.5}$) and ~40% of climate change-causing CO_2 emissions in recent years[1–3]. Historically, the health risks posed by such air pollution have been mediated by stringent environmental policies and emission standards focused on reducing end-of-pipe emissions from fossil fuel-fired power plants[4–6]. But increasingly, studies have pointed out the large health 'co-benefits' of reducing use of fossil fuels[7–17]. Specifically, prior studies have quantified the extent to which the energy transition entailed by international efforts to limit the increase in global mean temperature to well below 2 °C (ref. [18]) and to 'pursue efforts' to avoid a 1.5 °C increase[19] would also reduce air pollutant emissions[10,16,17]. Yet such health co-benefits are not ensured and may be unevenly distributed depending on details of regional climate–energy and clean air policies[5,13,14]. In particular, for the power sector, differences in the timing of changes, the management of existing generating infrastructure and the level of air pollution emissions standards may each result in large differences in the number and location of annual and cumulative air pollution deaths this century. Yet, despite enormous implications for human health and the overall benefits of climate change mitigation, there has been no comprehensive accounting of the sensitivity of public health outcomes to differences in unit-level management decisions in the global power sector.

Here, we develop a data-driven method for quantifying the fossil fuel- and biomass-fired power-related health co-benefits of different climate–energy and clean air policies, resolving scenarios at the level of individual generating units (Extended Data Fig. 1) and highlighting policies that yield the greatest health benefits while also meeting different climate goals. Details of our data sources, models, scenario design and analytic methods are provided in the Methods.

In summary, we first use a worldwide database of power plants, the Global Power Emissions Database (GPED)[20], to assess the health impacts of emissions from operating power plants by region, fuel type and capacity in 2010, as well as from identified super-polluting units[20]. We then calibrate the power unit fleet (supplementing new-built and retired units) and CO_2 and air pollution emissions for the period 2011–2018 using the real information (the GPED-2018; Supplementary Notes 1 and 2). On the basis of the disproportionalities between generating capacity and health impacts identified, we define three retirement strategies: one that allows power plants to operate for their historical expected lifetime before being replaced (40 years); one that prioritizes retirement of the most-polluting plants but slightly reduces the global average lifetime (~33 years); and one that again prioritizes retirement of the most-polluting plants but also substantially reduces the average lifetime to ~26 years to adapt stringent climate target (Supplementary Table 1 and Extended Data Fig. 2). Note that the regional electricity demand being met by biomass- and fossil fuel-fired plants we obtained from the Global Change Assessment Model (GCAM)[21] is unaffected by these retirement strategies; that is, we assume a coal-fired plant retired early is only replaced by a newer (more energy efficient and less polluting) coal plant to meet projected demand for coal electricity. In addition to retirement strategies, we also define three levels of pollution control technologies: the first in which pollution removal efficiencies of all operating units are kept to the 2018-level for reference (that is, reference); the second in which any units whose pollution removal efficiencies below the 2018 average are brought up to that average level of controls (that is, weak); and the last in which the best-available control technologies are deployed on all units (that, is strong; Supplementary Table 1).

On the basis of our developed top-down and bottom-up combined projections model that represents changes at the level

[1]Department of Earth System Science, Ministry of Education Key Laboratory for Earth System Modeling, Institute for Global Change Studies, Tsinghua University, Beijing, China. [2]Department of Earth System Science, University of California, Irvine, Irvine, CA, USA. [3]State Key Joint Laboratory of Environment Simulation and Pollution Control, School of Environment, Tsinghua University, Beijing, China. [4]Institute for Carbon Neutrality, Tsinghua University, Beijing, China. [5]These authors contributed equally: Dan Tong, Guannan Geng. ✉e-mail: qiangzhang@tsinghua.edu.cn; sjdavis@uci.edu

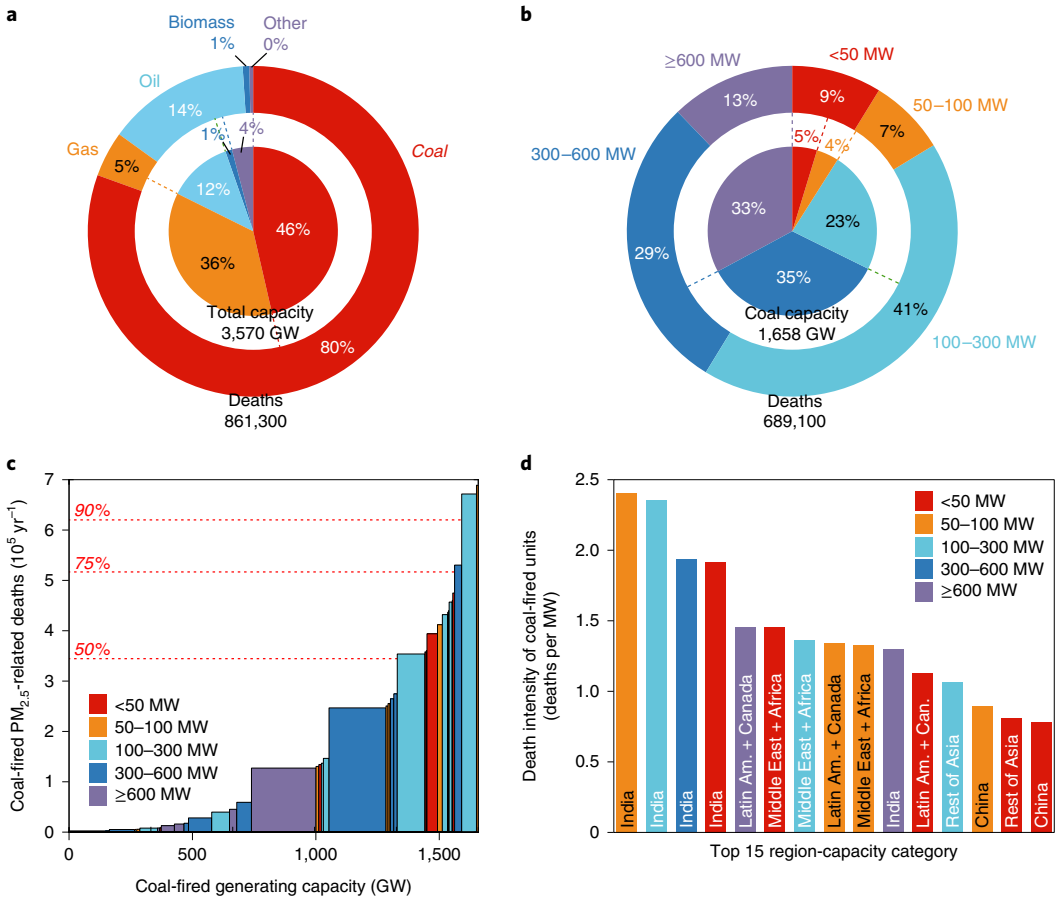

Fig. 1 | Shares of $PM_{2.5}$-related deaths from global power plants as of 2010. a, Shares of total generating capacity (inner pie chart) and $PM_{2.5}$-related deaths (outer ring chart) by fuel type (coal, gas, oil, biomass and other fuels such as waste, peat and coke oven gas). **b**, Shares of coal-fired power capacity (inner pie chart) and $PM_{2.5}$-related deaths (outer ring chart) by unit size (<50 MW, 50–100 MW, 100–300 MW, 300–600 MW and ≥600 MW). **c**, Rank ordering of coal-fired capacity by deaths per unit capacity (defined as 'death intensity') reveals large disparities (coloured by unit size) and the horizontal red lines indicate 50, 75 and 90% of total $PM_{2.5}$-related deaths induced by coal-fired power plants. **d**, The top 15 death intensity of coal-fired power units by region and unit size.

of individual generating units (Supplementary Notes 3–5), starting from 2018, we then model future unit-level power plant emissions (both CO_2 and air pollutants such as main $PM_{2.5}$ precursor species SO_2, NO_x and primary $PM_{2.5}$) under fixed socioeconomic development (the Shared Socioeconomic Pathways, SSPs: SSP2) with a range of climate mitigation scenarios[22] that span four levels of climate ambition (Representative Concentration Pathways, RCPs: 1.9, 2.6, 4.5 and 6.0 W m^{-2} of radiative forcing) and each of the three different retirement strategies (historical, performance-based and early retirement) and three stringencies of pollution controls (reference, strong and weak). It is noted that the deployment of carbon capture and storage (CCS) has requirements for impurities in flue gas streams (air pollution concentrations) to lower solvent degradation[23–26]. Therefore, power plants with CCS should inherently have a relatively high control level, which is also comprehensively modelled in our emission projections. Finally, we evaluate the global health impacts of $PM_{2.5}$ air pollution of our scenarios using the chemical transport model GEOS-Chem[27] and the epidemiological concentration–response (*C–R*) functions (the Global Exposure Mortality Model, GEMM)[28].

Power-related health impacts

We estimate that there were 7.30 million premature deaths related to $PM_{2.5}$ pollution in 2010 (our baseline year since most of the global climate scenarios begin in that year; 95% confidence interval (CI), 6.84–7.74 million). Of this global total, 12% or 861,300 (95% CI, 811,600–909,600) deaths were related to emissions from global fossil fuel- and biomass-fired power plants in 2010 (Supplementary Table 2). There are large disproportionalities between these deaths and the fuel type and size of electricity generators producing the air pollution (Fig. 1). For example, coal-fired plants account for 46% (1,658 GW) of the world's generating capacity (totally 3,570 GW; Supplementary Table 3) in the GPED-2010 but 80% (689,100; 95% CI, 646,300–727,300) of power-related air pollution deaths (red in Fig. 1a; Supplementary Table 4). Further, among coal-fired plants, smaller capacity units (<100 MW) represented only 9% of generating capacity but accounted for 16% of $PM_{2.5}$-related deaths (113,100; 95% CI, 105,900–119,500; red and orange in Fig. 1b), while the largest plants (≥600 MW) represented 33% of generating capacity (545 GW) but caused only 13% (89,800; 95% CI, 83,400–95,500) of deaths (purple in Fig. 1b).

However, these global totals mask substantial disparities in the emission intensities of developed and developing countries; in many countries the disproportionalities between smaller capacity, coal-fired units and related air pollution deaths are even larger. Over 40% of the deaths (~300,000) were related to coal-fired plants that represent <10% of all coal-fired capacity (Fig. 1c), mainly small (<100 MW) and super-polluting units in low-income and emerging economies such as India, the Middle East and Africa (Fig. 1d). Further evaluation on all identified coal super-polluting units[20]

(single- or multi-pollutants) again reflects such regional disproportionalities (Extended Data Fig. 3) and >90% of $PM_{2.5}$ deaths related to global coal super-polluting units (341,200 in total) occurred in low-income and emerging economies (Supplementary Table 5). In contrast, regulation of coal-fired power plants in the developed regions (for example, the United States and Europe) was largely effective in protecting people from dying due to $PM_{2.5}$ air pollution.

Further, from 2010 to 2018, the disparities of health impacts between developed and emerging economies enlarged due to the continuous controls and coal retirements in the developed regions, as well as the ever-lax regulations in low-income and emerging economies except China, which benefitted from an 'ultra-low' emission standard in recent years[5] (Supplementary Table 6). With the advanced controls of new-built units and retrofit/retirement of old units during 2010–2018, as a result, the shares of capacity and deaths related to super-polluting units of 2010 substantially declined by 2018. For example, the remaining 8.0% of super-polluting coal capacity (12.3% in 2010) contributed 18.5% of coal deaths in the 'Rest of Asia' in 2018 (72.1% in 2010; Supplementary Table 5). The still-existing disproportionalities in generating capacity and health impacts during 2010–2018, in addition to newly identified super-polluting units, are used to define the 'performance-based' strategy that prioritizes power plant retirements according to the estimated air pollution deaths caused per unit of generating capacity (death intensity).

Health benefits of tailored retirement strategies

Demand for electricity from biomass- and fossil fuel-fired plants increases during 2018–2030, after which such demand without CCS decreases only in scenarios likely to avoid increasing global mean temperatures by either 2.0 or 1.5 °C (RCP2.6 and RCP1.9, respectively; Supplementary Figs. 1 and 2). In turn, given steadily increasing and aging populations (Supplementary Fig. 3), annual air pollution deaths also increase until 2030 in many scenarios (Fig. 2). If plants retire as historically and pollution controls are weak, annual $PM_{2.5}$-related deaths in 2030 reach 0.93 million and 1.19 million in RCP1.9 and RCP6.0, respectively (RCP2.6 and RCP4.5 share the same electricity demand pathways as RCP6.0 during 2018–2030; small and lighter circles in Fig. 2a; hereinafter we refer to this RCP6.0 scenario as the baseline). Reference controls will further worsen the health burdens (reaching 1.05 million and 1.28 million in RCP1.9 and RCP6.0 in 2030, respectively; Supplementary Table 7).

Between 2030 and 2050, differences in $PM_{2.5}$-related deaths across climate scenarios grow: again assuming historical retirement and weak pollution controls, deaths in the baseline RCP6.0 reach about three times the 2010 levels in 2050 (2.18 million per year) while deaths are substantially 87% lower (291,900 per year) in RCP1.9 scenarios likely to avoid 1.5 °C of warming due to the combination of energy transition and CCS deployment (small and lighter grey and purple circles in Fig. 2b, respectively). In contrast to the health benefits of ambitious climate targets which occur mostly after 2030, the deployment of pollution control technologies—focusing on reducing the end-of-pipe emissions—can effectively and immediately lower pollution emission intensities (Fig. 2a, b). Indeed, widespread deployment of strong pollution controls in the near-term can mostly avoid increases in $PM_{2.5}$-related deaths in 2030 and 2050 even where climate mitigation is weak (RCP6.0). More than half of baseline $PM_{2.5}$-related deaths (60–68%) can be avoided by deployment of strong pollution controls regardless of retirement strategies in RCP4.5 and RCP6.0 as of 2050 (strong control group versus weak control group in Fig. 2b). By 2050, under the most strong scenario (RCP1.9 with early retirement and strong pollution control), there are significant emission reductions (−90% of SO_2, −82% of NO_x and −96% of $PM_{2.5}$ during 2010–2050; Supplementary Table 8) but not equivalent health benefits (185,300 premature deaths compared to 861,300 in 2010), implying future population increasing and aging notably swallow part of health benefits from air quality improvement, especially for the developing regions.

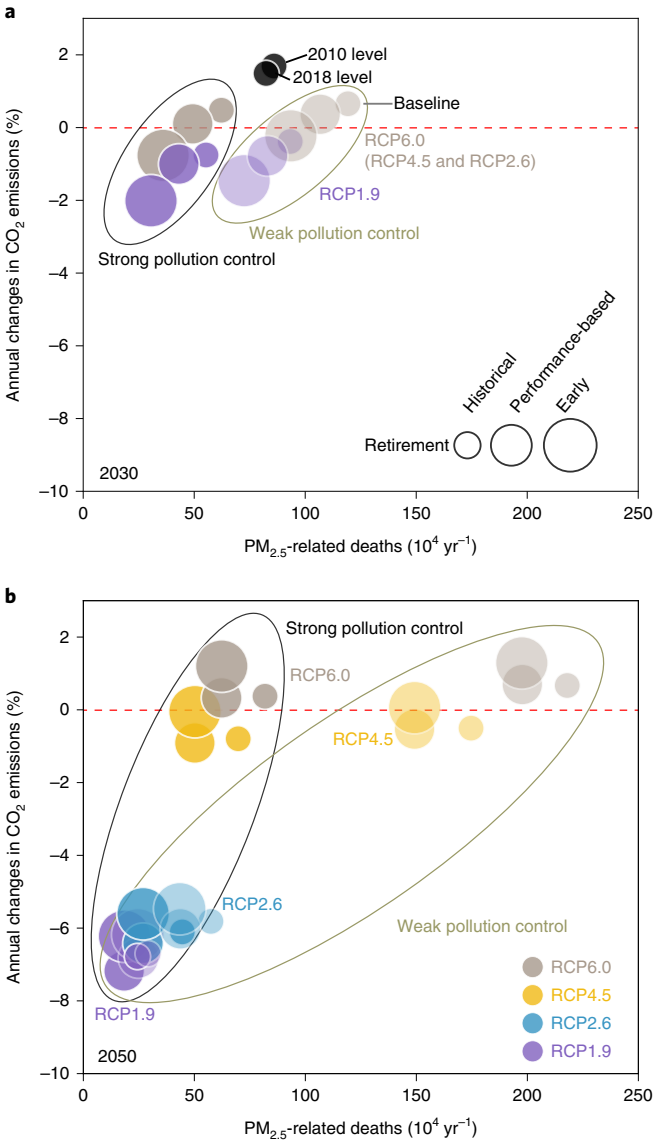

Fig. 2 | Mean annual change in CO_2 emissions and $PM_{2.5}$-related deaths. **a**,**b**, The relationship between annual average CO_2 reduction rate and $PM_{2.5}$-related deaths under the scenario assemble in 2030 (**a**) and 2050 (**b**), spanning four levels of climate ambition (RCP6.0, RCP4.5, RCP2.6 and RCP1.9), three different retirement strategies (historical, performance-based and early retirement) and two stringencies of pollution controls (strong and weak). The filled black circles in **a** show the mean annual change in CO_2 emissions during 2010–2015 (and 2010-level $PM_{2.5}$-related deaths) and 2010–2018 (and 2018-level $PM_{2.5}$-related deaths), respectively.

Annual changes in CO_2 emissions and $PM_{2.5}$-related deaths (also $PM_{2.5}$-related years of life lost; Extended Data Fig. 4) differ as a function of climate mitigation as well as the different pollution control stringencies and retirement strategies (Fig. 2; emission differences are shown in Extended Data Fig. 5 and Supplementary Table 8). For example, despite the different sign of annual changes in CO_2 emissions under RCP6.0 (weak mitigation, grey circles, CO_2 emissions still growing) and RCP1.9 (very strict mitigation, purple circles, annual emissions decreasing), $PM_{2.5}$-related deaths in 2030 are less

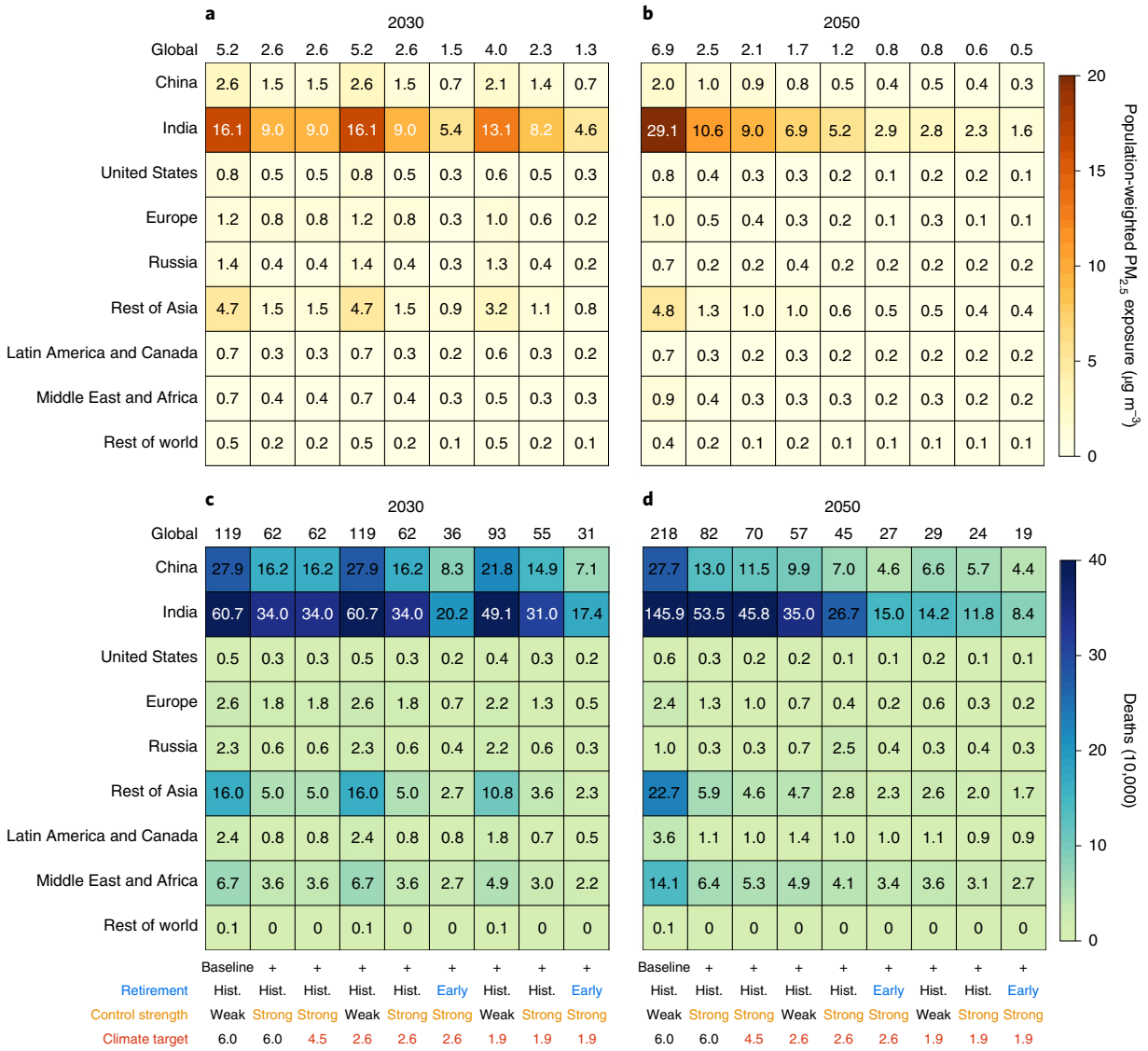

Fig. 3 | $PM_{2.5}$ exposures and $PM_{2.5}$-related deaths that are linked to emissions from global power plants. a,**b**, Regional $PM_{2.5}$ exposure in 2030 (**a**) and 2050 (**b**). **c**,**d**, $PM_{2.5}$-related premature mortality in 2030 (**c**) and 2050 (**d**) under a series of combined scenarios (climate ambitions, retirement strategies and stringencies of pollution controls). Hist., historical.

sensitive to climate pathway than to the stringency of pollution control and retirement strategies (indicated by horizontal distances between various circles in Fig. 2a). Therefore, if strong pollution control is implemented, retirement strategy can determine whether RCP6.0 or RCP1.9 have less power plant-related air pollution deaths (dark circles in Fig. 2).

However, by 2050 the effects of retirement strategies on modelled air pollution deaths have been narrowed because most of all the units operating before 2018—including identified super-polluting units—are replaced by the new units regardless of the retirement strategy. Meanwhile, the effects of CCS deployment on air pollution deaths are particularly observed under ambitious climate targets (for example, RCP1.9). Even under the weak control stringency scenario, the addition of air pollution control technologies through CCS deployment would substantially reduce the air pollution deaths. That is, almost all the power plant-installed CCS under all RCP1.9 scenarios have more similar performances on air pollution deaths as of 2050 (185,300–351,400 deaths in RCP1.9 versus 623,500–3.00 million deaths in RCP6.0; the reference scenarios are shown in Supplementary Table 7).

Regional disparities

Although global changes in CO_2 and air pollution emissions vary substantially across our scenarios (Supplementary Table 8), there are drastic regional disparities in air pollution and health impacts. For all the future scenarios, from 2030 to 2050, the disproportionalities of changes between air quality and $PM_{2.5}$-related deaths indicate where extra efforts are needed to offset the increasing size and age of the regional population (Fig. 3 and Supplementary Fig. 3). For example, during 2030–2050, 72% of the global air quality improvement (2.3–0.6 μg m^{-3}; the eighth columns in Fig. 3a,b) can only bring 56% of avoided pollution deaths (553,000–243,600 deaths; the eighth columns in Fig. 3c,d) under the ambitious climate target that successfully avoiding 1.5 °C of warming (RCP1.9).

In many future scenarios, both the overall number of deaths and the share occurring in low-income and emerging economies grow, such as in India, the Middle East and Africa. Most strikingly, $PM_{2.5}$-related deaths related to the power plant emissions in India almost quadruple between 2010 and 2050 under the baseline scenario (historical retirements and weak pollution controls). Moreover, in 2050, 90% of deaths in the baseline scenario occur in

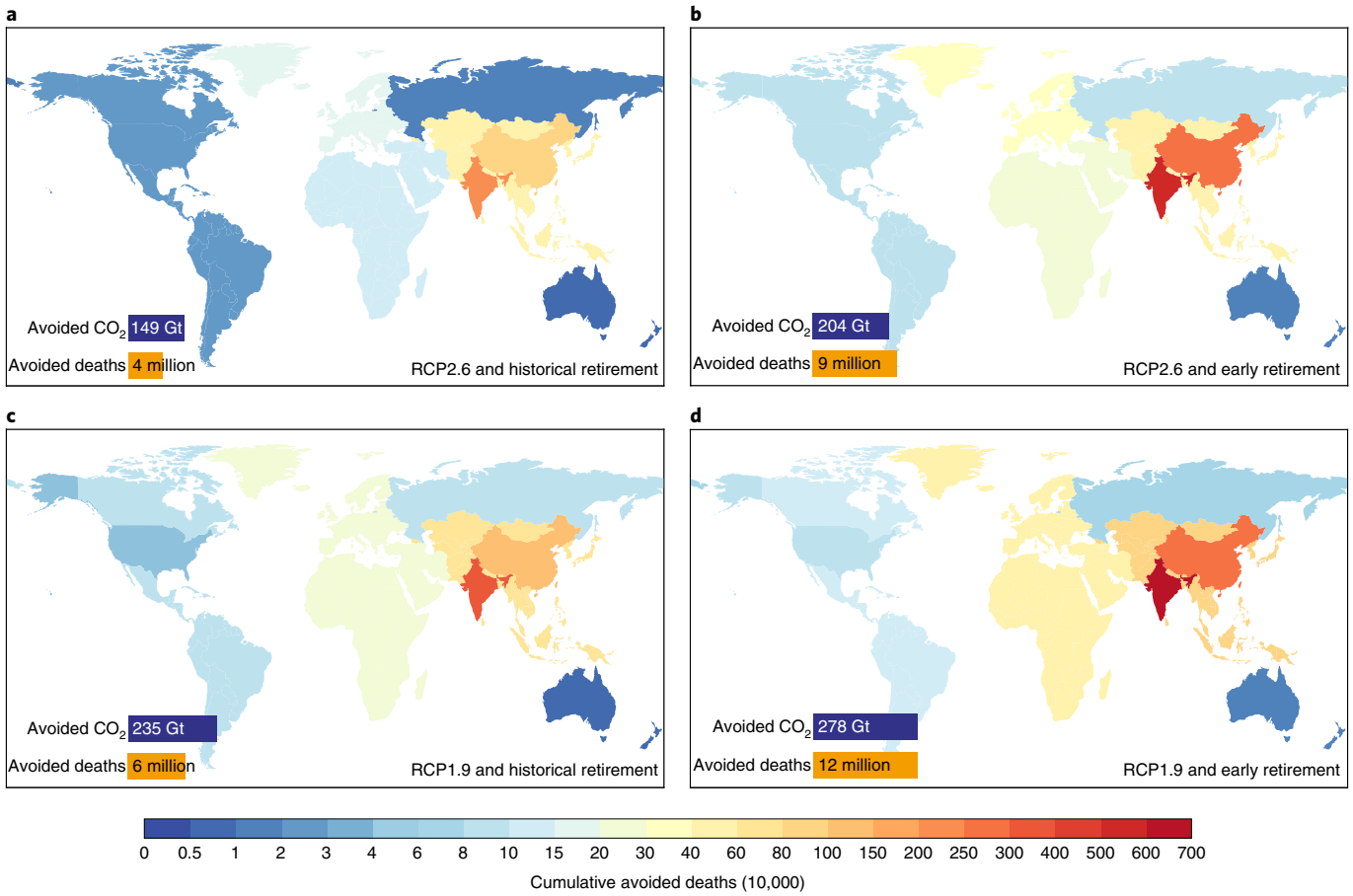

Fig. 4 | Cumulative avoided $PM_{2.5}$-related deaths and CO_2 emissions 2010–2050. a–d, Accumulative CO_2 mitigations and avoided $PM_{2.5}$-related deaths during 2010–2050 from RCP2.6 climate target with historical retirement (**a**), RCP2.6 climate target with early retirement (**b**), RCP1.9 with historical retirement (**c**) and RCP1.9 climate target with early retirement (**d**), compared with the RCP6.0 target with historical retirement. Note that all scenarios here deployed the strong pollution control technologies.

Asia (1.96 million of 2.18 million; first column of Fig. 3d) due to rapid projected growth in both fossil fuel-fired electricity demand and population. In addition, the Middle East and Africa make up more than half of $PM_{2.5}$-related deaths outside Asia in the baseline scenario in 2050 (65%, 140,700 deaths in 2050) despite comparable population-weighted $PM_{2.5}$ exposure in either the United States or Europe (first column of Fig. 3b).

Strategic power plant retirements (either performance-based or early retirements) especially help in low-income and emerging economies whose power-generating units are young but which tend to have smaller generating capacities, lower efficiencies and higher pollution emissions per unit capacity (Fig. 1c). For example, in China and India, 77,200 (~52% of avoided deaths in RCP1.9 with strong pollution control) and 136,100 (44%) $PM_{2.5}$-related deaths in 2030 could be avoided by early retirement and replacement of generators, respectively (the last two columns in Fig. 3c). Our additional coal super-polluting isolated simulation further shows that, strategic power plant retirements under RCP1.9 with strong pollution control (early retirement and strong pollution controls) would rapidly and entirely eliminate the identified super-polluting units by 2030 compared to historical retirement and under the historical retirement there still exist 5.2% of coal super-polluting capacity whose ages are young, far from 'aged out', but electric efficiencies and end-of-pipe controls are poor by 2030, which could still contribute 29.5% of $PM_{2.5}$-related deaths in 2030 (Supplementary Table 5). The early (and performance-based) retirement of identified super-polluting units through strategic power plant retirements, especially for low-income and emerging economies, could substantially reduce the health burden under the same climate–energy and clean air pathway.

Cumulative health benefits

Although ambitious climate mitigations under RCP2.6 or RCP1.9 reach low levels of annual air pollution deaths by 2050, large numbers of deaths can be avoided in the intervening decades by targeted early retirement and replacement of super-polluting power plants (Fig. 4). For example, comparing RCP6.0 and RCP2.6, both with strong pollution controls and power plants retiring as they have historically, we estimate a cumulative 149 Gt of CO_2 emissions and 4 million air pollution deaths would be avoided between 2010 and 2050 (Fig. 4a). However, when coupled with a strategy of early retirement, the cumulative avoided CO_2 emissions and deaths increase by 37 and 125% to 204 Gt and 9 million, respectively (Fig. 4b). The additional CO_2 emissions avoided are due to improved energy efficiency of replacement power plants (climate scenarios dictate the demand for biomass- or fossil fuel-electricity but newer plants may be considerably more energy efficient).

The cumulative benefits of strategic retirements under the even-more-ambitious RCP1.9 are also large: 18% more CO_2 emissions and 100% more deaths avoided (from 235 $GtCO_2$ and 6 million deaths avoided to 278 Gt and 12 million deaths avoided; Fig. 4c,d). And as suggested by the red areas of the maps in Fig. 4, millions of these avoided deaths are concentrated in India, China and the Rest of Asia region. In fact, 45% of the $PM_{2.5}$-related deaths

under the RCP1.9+early retirement scenario is occurred in India and four-fifths of the rest avoided deaths are in either China or the Rest of Asia region.

Discussion

Our detailed and dynamic analysis of climate, pollution and health impacts from the future power systems at the level of individual generating units reveals that air pollution deaths are not an automatic and fixed co-benefit of all climate mitigation. Rather, pollution controls and strategic retirements of the most-polluting and harmful power plants may ultimately determine the extent to which health co-benefits are realized. This is especially clear when considering the different time scales of these various technological and policy interventions: whereas the evolution of electricity systems as a result of long-term climate policies may greatly diminish annual air pollution deaths by 2050, pollution controls and retirement/replacement decisions could have equally large effects on annual deaths over the next decade, leading to millions of cumulative avoided deaths, especially in Asia. The elimination of super-polluting units especially in China, India and the Rest of Asia would have a disproportionately large health benefit in those regions and worldwide and international cooperation to support such retirements/retrofits is important. Our analysis on health co-benefits of climate change mitigation policy implies different and targeted policy implications compared to more recent results[29,30].

Several important uncertainties and limitations apply to our findings. First, the trajectory of future emissions depicted in our scenarios reflects an assumption that existing electricity-generating units either 'age out' at historical retirement schedules or else are strategically targeted for retirement and replacement with more efficient and lower-emitting units. In addition, the fuel-specific electricity demand projected from the GCAM model implies its underlying specific-power plants assumptions[31]. The scenario design of this study on different strategic retirements may induce uncertainty by ignoring the feedback of retirement strategy on the changes of cost and power demand (Supplementary Note 4 gives detailed discussion and evaluation). Second, the current resolutions of Integrated Assessment Models (IAMs) are relatively coarse compared to our unit-level emission projections model and the base year of these IAMs is far to present for 10 years and may be greatly different from current development. Only one model was used in this study (GCAM), while different IAMs have various projections on future electricity demand and electricity supply structure. All of these uncertainties would affect the estimates of energy consumption, final pollution emissions and premature deaths and detailed discussions are presented in Supplementary Note 4. Third, given unavailability of more detailed planning information, we project that emissions of newly built units will occur at the same locations as retired ones. Larger health benefits might be obtained if we instead optimized the siting of newly built units[32]. Fourth, the degree of air quality and health benefits is subjected to the zero-out method we used and the effects of future meteorological conditions. Several sensitivity simulations we conducted indicate relatively small effects on the power-related pollution estimates (Supplementary Note 6). In contrast, future meteorological conditions will be influenced by climate change and remain highly uncertain, although several studies have projected that meteorological changes may in fact worsen air quality in key regions such as China[33], such that we may underestimate the deaths avoided by reducing air pollution emissions.

Regardless, by modelling differences in emissions and deaths at the unit level, our results add important nuance to policy-relevant discussions of health co-benefits of climate change mitigation by showing that realizing such benefits often depends on supplementary programmes to deploy pollution control technologies and to target super-polluting units for retirement and replacement, especially for coal power elimination. Even assuming successful climate change mitigation and strong pollution controls, implementing our data-driven approach to targeting super-polluting units for retirement and replacement could save millions of lives worldwide by the middle of the century.

Online content

Any methods, additional references, Nature Research reporting summaries, source data, extended data, supplementary information, acknowledgements, peer review information; details of author contributions and competing interests; and statements of data and code availability are available at https://doi.org/10.1038/s41558-021-01216-1.

Received: 30 June 2020; Accepted: 11 October 2021;
Published online: 29 November 2021

References

1. Lelieveld, J., Evans, J. S., Fnais, M., Giannadaki, D. & Pozzer, A. The contribution of outdoor air pollution sources to premature mortality on a global scale. *Nature* **525**, 367–371 (2015).
2. Jackson, R. B. et al. Global energy growth is outpacing decarbonization. *Environ. Res. Lett.* **13**, 120401 (2018).
3. Tong, D. et al. Committed emissions from existing energy infrastructure jeopardize 1.5 °C climate target. *Nature* **572**, 373–377 (2019).
4. Tong, D. et al. Current emissions and future mitigation pathways of coal-fired power plants in China from 2010 to 2030. *Environ. Sci. Technol.* **52**, 12905–12914 (2018).
5. Wu, R. et al. Air quality and health benefits of China's emission control policies on coal-fired power plants during 2005–2020. *Environ. Res. Lett.* **14**, 094016 (2019).
6. Ou, Y., West, J. J., Smith, S. J., Nolte, C. G. & Loughlin, D. H. Air pollution control strategies directly limiting national health damages in the US. *Nat. Commun.* **11**, 957 (2020).
7. West, J. J. et al. Co-benefits of mitigating global greenhouse gas emissions for future air quality and human health. *Nat. Clim. Change* **3**, 885–889 (2013).
8. Driscoll, C. T. et al. US power plant carbon standards and clean air and health co-benefits. *Nat. Clim. Change* **5**, 535–540 (2015).
9. Buonocore, J. J. et al. Health and climate benefits of different energy-efficiency and renewable energy choices. *Nat. Clim. Change* **6**, 100–105 (2016).
10. Shindell, D. T., Lee, Y. & Faluvegi, G. Climate and health impacts of US emissions reductions consistent with 2 °C. *Nat. Clim. Change* **6**, 503–507 (2016).
11. Millstein, D., Wiser, R., Bolinger, M. & Barbose, G. The climate and air-quality benefits of wind and solar power in the United States. *Nat. Energy* **2**, 17134 (2017).
12. Silva, R. A. et al. Future global mortality from changes in air pollution attributable to climate change. *Nat. Clim. Change* **7**, 647–651 (2017).
13. Peng, W. et al. Managing China's coal power plants to address multiple environmental objectives. *Nat. Sustain.* **1**, 693–701 (2018).
14. Shindell, D., Faluvegi, G., Seltzer, K. & Shindell, C. Quantified, localized health benefits of accelerated carbon dioxide emissions reductions. *Nat. Clim. Change* **8**, 291–295 (2018).
15. Luderer, G. et al. Environmental co-benefits and adverse side-effects of alternative power sector decarbonization strategies. *Nat. Commun.* **10**, 5229 (2019)..
16. Shindell, D. & Smith, C. J. Climate and air-quality benefits of a realistic phase-out of fossil fuels. *Nature* **573**, 408–411 (2019).
17. Scovronick, N. et al. The impact of human health co-benefits on evaluations of global climate policy. *Nat. Commun.* **10**, 2095 (2019).
18. Rogelj, J. et al. Paris Agreement climate proposals need a boost to keep warming well below 2 °C. *Nature* **534**, 631–639 (2016).
19. Rogelj, J. et al. in *Special Report on Global Warming of 1.5 °C* (eds Masson-Delmotte, V. et al.) Ch. 2 (IPCC, WMO, 2018).
20. Tong, D. et al. Targeted emission reductions from global super-polluting power plant units. *Nat. Sustain.* **1**, 59–68 (2018).
21. Luckow, P., Wise, M. A., Dooley, J. J. & Kim, S. H. Large-scale utilization of biomass energy and carbon dioxide capture and storage in the transport and electricity sectors under stringent CO_2 concentration limit scenarios. *Int. J. Greenh. Gas Control* **4**, 865–877 (2010).
22. O'Neill, B. C. et al. A new scenario framework for climate change research: the concept of Shared Socioeconomic Pathways. *Clim. Change* **122**, 387–400 (2014).
23. Rao, A. B. et al. Evaluation of potential cost reductions from improved amine-based CO_2 capture systems. *Energy Policy* **34**, 3765–3772 (2006).
24. van Horssen, A. et al. *The Impacts of CO_2 Capture Technologies in Power Generation and Industry on Greenhouse Gases Emissions and Air Pollutants in the Netherlands* (TNO and Univ. of Utrecht, 2009); https://www.rivm.nl/bibliotheek/digitaaldepot/BOLK_II_CCS_Final-Version%20UPDATE%2028-07-2010.pdf

25. *Air Pollution Impacts from Carbon Capture and Storage (CCS)* EEA Technical Report No. 14/2011 (European Environment Agency, 2011); https://www.eea.europa.eu/publications/carbon-capture-and-storage
26. Koornneef, J. et al. *Carbon Dioxide Capture and Air Quality: Chemistry, Emission Control, Radioactive Pollution and Indoor Air Quality* (InTech, 2011); https://www.intechopen.com/chapters/16320
27. Bey, I. et al. Global modeling of tropospheric chemistry with assimilated meteorology: model description and evaluation. *J. Geophys. Res. Atmos.* **106**, 23073–23095 (2001).
28. Burnett, R. et al. Global estimates of mortality associated with long-term exposure to outdoor fine particulate matter. *Proc. Natl Acad. Sci. USA* **115**, 9592–9597 (2018).
29. Rauner, S. et al. Coal-exit health and environmental damage reductions outweigh economic impacts. *Nat. Clim. Change* **10**, 308–312 (2020).
30. Sampedro, J. et al. Quantifying the reductions in mortality from air-pollution by cancelling new coal power plants. *Energy Clim. Change* **2**, 100023 (2021).
31. Fofrich, R.A. et al. Early retirement of power plants in climate mitigation scenarios. *Environ. Res. Lett.* **15**, 094064 (2020).
32. Sergi, B. J. et al. Optimizing emissions reductions from the U.S. power sector for climate and health benefits. *Environ. Sci. Technol.* **54**, 7513–7523 (2020).
33. Hong, C. et al. Impacts of climate change on future air quality and human health in China. *Proc. Natl Acad. Sci. USA* **116**, 17193–17200 (2019).

Methods

Unit-based emission projections. The GPED we previously developed[20] contains unit-based information (for example, unit capacity, start year of operation, technologies in place for desulfurization, denitration and dust removal) of fossil fuel- and biomass-burning power generators in service as of 2010, as well as CO_2 and pollutant emissions (SO_2, NO_x and primary $PM_{2.5}$). We first update the GPED—by integrating the latest World Electric Power Plants Database and local datasets—to track regional power unit development (new-built and retired unit information) and CO_2 and pollutant emissions during 2011–2018 (GPED-2018; Supplementary Notes 1 and 2). Starting from the GPED-2018, a unit-based top-down and bottom-up combined emission projection model that represents future changes at the level of individual units is developed for this study to estimate future fossil fuel- and biomass-burning power plant emissions worldwide through 2050, which is extended and adapted on the basis of the unit-based emission projection model developed for China's coal-fired power plants[4].

The projection model is designed to simulate power plant fleet turnover by tracking the lifespan of each power generation unit, which is modelled by region (totally 31 regions; Supplementary Table 9) and fuel type (coal, natural gas, oil, biomass and other fuels such as waste, peat and coke oven gas; Supplementary Table 10) on an annual basis (Extended Data Fig. 1). Within each region and fuel type, for a given year, the model first estimates the power supply capability of in-fleet units (suppliable power generation) after implementing retirement policies, which is determined by the operating-unit installed capacity and 2018-year capacity factors. The model then estimates the power supply gap under the certain fuel-type-specific electricity demand provided by future energy scenarios and fills the gap using new-built same-fuel-type generating units. Note that the regional electricity demand being met by biomass- and fossil fuel-fired plants is unaffected by these retirement strategies. For example, we assume a coal-fired plant retired is only replaced by a newer (more energy efficient and less-polluting) coal plant to meet projected demand for coal electricity. By assuming different lifespan and retirement polices for each unit in different mitigation pathways, the power plant fleet structure then changes as a result of the retirement of old units and the construction of new units. We then model the changes in emission factors at the unit level by considering the evolution of end-of-pipe control technologies under different pollution control strength assumptions (Supplementary Note 3).

Scenario design. Climate mitigation scenarios, coupled with different retirement strategies and stringencies of pollution controls, are specifically considered as future mitigation options for global fossil fuel- and biomass-burning power plants. We first derive future fossil fuel- and biomass-burning electricity demand under a range of climate mitigation scenarios from the GCAM[21] (http://www.globalchange.umd.edu/gcam/). The GCAM is a global IAM that represents the behaviour of, and interactions between, five systems: the energy system, water, agriculture and land use, the economy and the climate. A new scenario framework, combining pathways of future radiative forcing and their associated climate changes (RCPs)[34] with alternative pathways of socioeconomic development (SSP1–5)[22], is developed for climate change research. Each SSP–RCP combination represents an integrated scenario of future climate and societal change, which can be used to investigate the mitigation effort required to achieve that particular climate outcome, the possibilities for adaptation under that climate outcome and assumed societal conditions and the remaining impacts on society or ecosystems[35]. To eliminate the effects from the socioeconomic conditions, we combine moderate SSP narrative (SSP2) with four levels of RCP scenarios (6.0, 4.5, 2.6 and 1.9 W m^{-2}) as our climate–energy scenarios. In detail, the GCAM model directly provides the region- (31 regions), fuel- and with/without CCS-specific electricity demands every 10 yr from 2010 to 2050. We linearly interpolate regional power demand at every 10-yr interval to obtain future annual demand (2018–2050). We also proportionally adjust the power generation demand from GCAM model due to the inconsistency between real historical electricity and projections from the GCAM in the year of 2018. In addition, the energy consumption in the power sector provided by the GCAM is not used in our study, which would be derived through our unit-level projections model (power generation multiplied by fuel consumption rate).

Various retirement strategies would alter the power plant fleet structure and further influence the future operating units' emission characteristics. Historically, statistical results show that fossil fuel-fired units generally operate for ~40 yr globally, which reflects the decision to retire a unit or power plant with the economic consideration of operating costs, replacement costs and revenues[36]. Prior studies highlight the substantial decreases of the lifetime or operation of existing energy infrastructure to meet the 1.5 °C climate target. It is estimated that even if no new plants are built, the lifetimes of existing units as of 2017 are reduced to ~35 yr in a well-below 2 °C scenario or 20 yr in a 1.5 °C scenario[37]. Apart from reducing the lifetimes of existing units to adapt strict climate targets, our study also highlights large disparities in health impacts at the unit level[20]. Super-polluting units (higher emission intensity than regional mean) that we previously defined represent larger undesirable emissions that should be reduced first. We therefore design three different retirement strategies to assess the health benefits from strategic power plant retirements, including historical, performance-based and early retirements (Supplementary Table 1). Historical retirement allows power plants to operate for their historical expected lifetime before being replaced (40 yr). Performance-based retirement prioritizes retirement of the most-polluting plants but slightly reduces the global average lifetime (~33 yr) and all the current operating capacities specifically are linearly retired from 2018 to 2050. More aggressively, early retirement again prioritizes retirement of the most-polluting plants but also substantially reduces the average lifetime to ~26 yr (all the current operating capacities are linearly retired from 2018 to 2030). The detailed description on the retirement function development at the individual level is shown in Supplementary Note 4.

The efficiencies of end-of-pipe controls would determine the ultimate emission level. By 2018, operating units, especially in the developing regions except China, are in poor pollution controls. We thus design three stringencies of pollution control in response to air pollution induced by the power sector and possible implemented clean power actions (Supplementary Table 1). The reference control reflects the future emission changes that there is no any air pollution control policy. Under the reference scenario, we assume the pollution removal efficiencies of all the operating power units will remain at the 2018-level (Supplementary Tables 11 and 12) and new units to fill the power supply gap will be built with pollution controls whose removal efficiency equals the mean removal efficiency of in-fleet units (Supplementary Tables 13 and 14). Weak and strong controls refer to lax and strict environmental regulations, respectively. Under the weak control strength, we assume that all the operating power units whose pollution removal efficiencies are below the 2018 average are brought up to that average level of controls and new units to fill the power supply gap will be built with advanced combustion technology and relatively high-efficient control measures whose removal efficiency equals the mean removal efficiency of units built in 2018. Strong control strength assumes that all the operating power units whose removal efficiencies are lower than the best-available control technologies will be gradually retrofitted to meet the best level derived from the related documents such as in the European Union and China[38,39]. And new units will be built with the most highly efficient combustion technologies and control measures whose removal efficiency equals that of the best-available technologies.

Pollution controls under each stringency applied to the same fuel type with CCS and without CCS are particularly different because strict air pollution concentrations are required for impurities in flue gas streams (air pollution concentrations) to lower solvent degradation[15,22–25,40]. For power plants with CCS device, there are large ranges for air pollution concentrations[22–25] and our estimates for the requirement of average control efficiencies are, respectively, 80–95%, 60–85% and 96–99.3% for SO_2, NO_x and $PM_{2.5}$. Therefore, power units with CCS device are modelled with additional air pollution controls if their control efficiencies are less than our assumption. That is, pollution control levels are not only determined by the local environmental policies but also affected by the penetration rates of CCS deployment.

Additionally, the differences of retrofit process and the removal efficiency of best-available technology among different regions (for example, between developing countries and developed counties) and fuel types are comprehensively considered according to their emission characteristics, previous environmental policies and future possible environmental challenges. The retrofit order is basically the reverse of the retirement order but low-efficient controls is our priority. The description of retrofit functions at the individual level is shown in Supplementary Note 5.

Estimates of $PM_{2.5}$ concentrations. The global GEOS-Chem model[27] is used to calculate the fractional contribution of global power plant-related emissions to global $PM_{2.5}$ concentrations at the grid level. Determined by the horizontal resolution of GEOS-Chem, the fractional contributions are calculated on a 2° latitude × 2.5° longitude grid. These spatially varying fractions are then multiplied by the 0.1° × 0.1° global annual mean $PM_{2.5}$ concentrations taken from GBD2013 in the year of 2010[41] to get power plant-related $PM_{2.5}$ concentrations. The 0.1° × 0.1° GBD2013 grid cells are applied with the simulated fraction from the 2° × 2.5° grid cells they fall in.

We use the GEOS-Chem v.11-01 driven by assimilated meteorological fields from the NASA Global Modeling and Assimilation Office's Modern-Era Retrospective analysis for Research and Applications v.2 (MERRA-2)[42]. The model has a horizontal resolution of 2° × 2.5° and 47 vertical layers. The model is run with full O_x–NO_x–CO–VOC–HO_x chemistry and includes sulfate–nitrate–ammonium[43,44], primary[45] and secondary[46] carbonaceous aerosols, mineral dusts[47,48] and sea-salts[49,50]. Sulfate–nitrate–ammonium is modelled by the ISOROPLA-II thermodynamical equilibrium. Primary organic aerosols are simulated as primary organic carbon in the model and then multiplied by 1.8 to account for the oxygen molecules contained when calculating ambient $PM_{2.5}$ concentrations. Secondary organic aerosols are predicted on the basis of rate constants and aerosol yield parameters determined from laboratory chamber studies[46,51]. The aerosol simulations have been extensively evaluated using ground-based measurements[44,47,52] and aircraft measurements[53,54].

The global sectoral anthropogenic emissions of NO_x, SO_2, CO, NMVOC, NH_3, BC and OC are used to drive GEOS-Chem simulations, which are derived in different ways. Except for emissions from the power sector, monthly gridded NO_x, SO_2, CO, NH_3, BC and OC emissions at 0.1° × 0.1° resolution from other sectors (industry, transport, residential and agriculture) as of 2010 are directly obtained

from the HTAP_V2 dataset[55]. Annual gridded emissions from the power sector developed in this work are converted to monthly gridded emissions at 0.1°×0.1° resolution in proportion to the monthly emissions grid maps of the energy sector from the HTAP_V2 dataset for 2010. These high-resolution emissions (0.1°×0.1° resolution) are automatically remapped to 2°×2.5° in the model simulations. It is noted that annual emissions from the power sector in 2010 are allocated to the 0.1°×0.1° grids according to units' geolocations. Due to very little contribution of the power sector to anthropogenic NMVOC emissions, we assume that NMVOC emissions are held constant in all model simulations. Anthropogenic NMVOC emission are taken from the monthly RETRO inventory with speciated NMVOC emissions[56]. MEGAN emissions are used for biogenic NMVOC[57] and the monthly GFED3 dataset is used for the biomass-burning emissions[58]. Other individual emission sources, such as aircraft[43], shipping[59], soil NO_x (ref. [60]) and lightning NO_x (refs. [61–63]), are also included in the simulation. The simulations are conducted for the entire 2010 year with a 6-month spin-up starting from July 2009. The 24-h average $PM_{2.5}$ concentrations in the bottom layer of the model are taken to represent the ground-level concentrations.

We also evaluate the base model simulations against ground measurements of $PM_{2.5}$, ground measurements of aerosol optical depth (AOD), satellite-retrieved AOD and global burden of diseases (GBD) $PM_{2.5}$ fusion dataset in 2010 (Supplementary Note 7). In summary, our modelled AOD and $PM_{2.5}$ concentrations agree well with those datasets (Supplementary Figs. 4–7) and are comparable to other global simulation studies[1,64].

The zero-out approach is used to simulate the fractional contributions of global power plant-related emissions to $PM_{2.5}$ concentrations and related deaths (Supplementary Table 15 gives model simulation design). In particular, a base simulation contains global anthropogenic and natural emissions and the base case subtracts the global anthropogenic power plant-related emissions of NO_x, SO_2, CO, NH_3, BC and OC produced to derive the contributions of global power plants to the global $PM_{2.5}$ concentrations. That is, all regional emissions related to the power plants are shut off together in each simulation. The second set of base-year cases separately subtracts the anthropogenic power plant-related emissions produced within each of fuel types, capacity sizes and super-polluting units to derive the corresponding contributions of fuel type- and sized specific-power plants to the global $PM_{2.5}$ concentrations, as well as the contributions of identified super-polluting units. Similarly, the future scenarios to split global power plants-related contributions during 2011–2050 apply the same zero-out method as the base-year case. The zero-out approach used here may introduce additional uncertainties due to the nonlinear relationship between emissions and modelled $PM_{2.5}$ concentrations. In addition, future emissions from other sectors will change with the climate and environmental polices like the power sector, which may also introduce additional bias in estimating the fractional contribution of power sector. We therefore perform a set of sensitivity tests (Supplementary Note 6) and the results indicate that the uncertainties related to nonlinear effects are relatively small (Supplementary Figs. 8 and 9).

$PM_{2.5}$-related mortality and years of life lost estimates. Premature mortality attributable to ambient $PM_{2.5}$ exposure is commonly used as the health burden indicator in policy evaluations of health co-benefits[65]. Attributable mortalities from outdoor $PM_{2.5}$ exposures are widely estimated by applying the Integrated Exposure–Response model (IER)[65] developed for the GBD study[66]. However, limited by chronic studies of outdoor $PM_{2.5}$ and mortality in areas with relatively low concentrations (<35 μg m^{-3}), at high $PM_{2.5}$ concentrations the previous IER functions provide the relationships between chronic exposure and attributable deaths (called *C*–*R* relationships) by $PM_{2.5}$–mortality associations from non-outdoor $PM_{2.5}$ sources[65], which bias the estimates of disease burden attributable to $PM_{2.5}$ (ref. [28]). To resolve the uncertainties introduced by non-ambient $PM_{2.5}$–mortality associations, the GEMM is constructed by Burnett et al.[28] by incorporating outdoor air pollution data across the most of the global exposure range, especially the polluted areas (for example, China). We therefore apply the GEMM model to estimate the premature mortality attributable to chronic $PM_{2.5}$ exposures for this study. Meanwhile, years of life lost (YLL) attributable to ambient $PM_{2.5}$ exposure is a common indicator[67], which is also estimated in this study.

The GEMM is built for estimating $PM_{2.5}$-related non-accidental deaths and YLL due to non-communicable diseases (NCDs) and lower respiratory infections (LRIs), denoted as GEMM NCD + LRI. The GEMM NCD + LRI parameterizes the dependence of relative risk (RR) of NCD + LRI on concentrations (*C*):

$$\mathrm{RR}(C) = e^{\frac{\theta \times \ln\left(\frac{z}{\alpha}+1\right)}{1+e^{\left(-\frac{z-\mu}{\nu}\right)}}}, \text{ where } z = \max(0, C-2.4) \quad (1)$$

where *C* represents the $PM_{2.5}$ concentration (μg m^{-3}), *z* therefore represents the maximum of 0 and (*C* − 2.4), *e* represents Euler's number, and θ, α, μ and ν are parameters that determine the shape of *C*–*R* relationships. According to the parameters provided by the GEMM, RR of NCD + LRI are calculated by age for adults with every 5-yr interval from 25 yr to age >85 yr. Premature mortality and YLL for a population subgroup *p* (population by age and gender) in grid *i* ($M_{p,i}$) are further estimated:

$$M_{p,i} = P_{p,i} \times B_{p,c} \times \frac{\mathrm{RR}_p(C_i) - 1}{\mathrm{RR}_p(C_i)} \quad (2)$$

where $P_{p,i}$ represents the population amount for population subgroup *p* in grid *i*; $B_{p,c}$ represents the national average annual mortality incidence rate and YLL rate of NCD + LRI for population subgroup *p* and country/region *c* of grid *i*; $\mathrm{RR}_p(C_i)$ represents the relative risk of NCD + LRI for population subgroup *p* at the $PM_{2.5}$ exposure level of C_i. For the base year of 2010, national base mortality incidences and YLL rates are derived from the GBD2017 study[68] and GBD Results Tool[69] and demographic information by gender and age is obtained from the World Bank[70]. Gridded population distribution for 2010 with a horizontal resolution of 0.1°×0.1° is obtained from the Global Population for the World dataset[71]. Additionally, in this study, a distribution of 1,000 point estimates of θ calculated on the basis of the parameters provided by the GEMM is used to estimate the lower and upper bounds of a 95% CI around mean attributable mortality in the base year (2010).

For the health-related parameters in the years from 2011 to 2050, the future national/regional demographic information under each SSP pathway are derived from SSP Database-Version 2.0 developed by International Institute for Applied Systems Analysis[72] and harmonized with the base-year demographic structure (Supplementary Fig. 3). And future yearly gridded population distributions by age and gender with a horizontal resolution of 0.1°×0.1° are produced on the basis of the gridded population in the year of 2010 according the change rates of corresponding age- and gender-based population information from SSP Database. For the yearly base mortality incidences and YLL rates, we derive from the GBD2017 study and GBD Results Tool[69] for the years from 2011 to 2018 and future mortality incidences from the International Futures (IFs)[73] for the years 2018, 2030 and 2050. Here, we first derive the continuous yearly base mortality incidences during 2017–2050 from the IFs by linear interpolation. We then harmonize the base mortality incidences during 2017–2050 from IFs by linking the 2017 base mortality incidences to that from the GBD2017 study.

Data availability

The database GPED that supports the base-year findings of this study is available at http://www.meicmodel.org/dataset-gped.html. The base mortality incidences data during 2010–2018 are available at http://ghdx.healthdata.org/gbd-results-tool. The future base mortality incidences database is available at http://www.ifs.du.edu/ifs/frm_MainMenu.aspx. The future demographic structure database is available at https://tntcat.iiasa.ac.at/SspDb/dsd?Action=htmlpage&page=30. Emission data for other sectors are available at https://edgar.jrc.ec.europa.eu/emissions_data_and_maps. Emissions data of the power plants in scenarios produced that support the findings of this study are available at https://doi.org/10.5281/zenodo.5637476 (ref. [74]).

Code availability

The code of the GEOS-Chem model to simulate the global $PM_{2.5}$ concentrations is available at https://geos-chem.seas.harvard.edu/.

References

34. van Vuuren, D. P. et al. The Representative Concentration Pathways: an overview. *Clim. Change* **109**, 5–31 (2011).
35. O'Neill, B. C. et al. The Scenario Model Intercomparison Project (ScenarioMIP) for CMIP6. *Geosci. Model Dev.* **9**, 3461–3482 (2016).
36. Davis, S. J. & Socolow, R. H. Commitment accounting of CO_2 emissions. *Environ. Res. Lett.* **9**, 084018 (2014).
37. Cui, R. Y. et al. Quantifying operational lifetimes for coal power plants under the Paris goals. *Nat. Commun.* **10**, 4759 (2019).
38. Garbarino, E. et al. *Best Available Techniques (BAT) Reference Document for the Management of Waste from Extractive Industries in accordance with Directive 2006/21/EC* (Publications Office of the European Union, 2018);https://ec.europa.eu/jrc/en/publication/eur-scientific-and-technical-research-reports/best-available-techniques-bat-reference-document-management-waste-extractive-industries
39. *Guideline on Best Available Technologies of Pollution Prevention and Control for Thermal Power Plant* (Ministry of Ecology and Environment of the People's Republic of China, 2016); http://www.mee.gov.cn/gkml/hbb/bgth/201610/t20161009_365147.htm
40. Koornneef, J. et al. The impact of CO_2 capture in the power and heat sector on the emission of SO_2, NO_x, particulate matter, volatile organic compounds and NH_3 in the European Union. *Atmos. Environ.* **44**, 1369–1385 (2010).
41. Brauer, M. et al. Ambient air pollution exposure estimation for the global burden of disease 2013. *Environ. Sci. Technol.* **50**, 79–88 (2016).
42. Gelaro, R. et al. The Modern-Era Retrospective Analysis for Research and Applications, Version 2 (MERRA-2). *J. Clim.* **30**, 5419–5454 (2017).

43. Park, R. J., Jacob, D. J., Field, B. D., Yantosca, R. M. & Chin, M. Natural and transboundary pollution influences on sulfate–nitrate–ammonium aerosols in the United States: implications for policy. *J. Geophys. Res.* **109**, D15204 (2004).
44. Park, R. J., Jacob, D. J., Kumar, N. & Yantosca, R. M. Regional visibility statistics in the United States: natural and transboundary pollution influences, and implications for the Regional Haze Rule. *Atmos. Environ.* **40**, 5405–5423 (2006).
45. Park, R. J., Jacob, D. J., Chin, M. & Martin, R. V. Sources of carbonaceous aerosols over the United States and implications for natural visibility. *J. Geophys. Res.* **108**, 4355 (2003).
46. Liao, H., Henze, D. K., Seinfeld, J. H., Wu, S. & Mickley, L. J. Biogenic secondary organic aerosol over the United States: comparison of climatological simulations with observations. *J. Geophys. Res.* **112**, D06201 (2007).
47. Fairlie, D. T., Jacob, D. J. & Park, R. J. The impact of transpacific transport of mineral dust in the United States. *Atmos. Environ.* **41**, 1251–1266 (2007).
48. Zender, C. S., Bian, H. & Newman, D. Mineral dust entrainment and deposition (DEAD) model: description and 1990s dust climatology. *J. Geophys. Res.* **108**, 4416 (2003).
49. Alexander, B. et al. Sulfate formation in sea-salt aerosols: constraints from oxygen isotopes. *J. Geophys. Res.* **110**, D10307 (2005).
50. Jaeglé, L., Quinn, P. K., Bates, T. S., Alexander, B. & Lin, J. T. Global distribution of sea salt aerosols: new constraints from in situ and remote sensing observations. *Atmos. Chem. Phys.* **11**, 3137–3157 (2011).
51. Seinfeld, J. H. & Pankow, J. F. Organic atmospheric particulate material. *Annu. Rev. Phys. Chem.* **54**, 121–140 (2003).
52. Pye, H. O. T. et al. Effect of changes in climate and emissions on future sulfate–nitrate–ammonium aerosol levels in the United States. *J. Geophys. Res.* **114**, D01205 (2009).
53. Heald, C. L. et al. A large organic aerosol source in the free troposphere missing from current models. *Geophys. Res. Lett.* **32**, L18809 (2005).
54. van Donkelaar, A. et al. Analysis of aircraft and satellite measurements from the Intercontinental Chemical Transport Experiment (INTEX-B) to quantify long-range transport of East Asian sulfur to Canada. *Atmos. Chem. Phys.* **8**, 2999–3014 (2008).
55. Janssens-Maenhout, G. et al. HTAP_v2.2: a mosaic of regional and global emission grid maps for 2008 and 2010 to study hemispheric transport of air pollution. *Atmos. Chem. Phys.* **15**, 11411–11432 (2015).
56. Bolshcer, M. et al. *RETRO Deliverable D1-6* (RETRO Documentation, 2007).
57. Guenther, A. B. et al. The Model of Emissions of Gases and Aerosols from Nature version 2.1 (MEGAN2.1): an extended and updated framework for modeling biogenic emissions. *Geosci. Model Dev.* **5**, 1471–1492 (2012).
58. van der Werf, G. R. et al. Global fire emissions and the contribution of deforestation, savanna, forest, agricultural, and peat fires (1997–2009). *Atmos. Chem. Phys.* **10**, 11707–11735 (2010).
59. Wang, Y., Jacob, D. J. & Logan, J. A. Global simulation of tropospheric O_3-NO_x-hydrocarbon chemistry: 1. Model formulation. *J. Geophys. Res.* **103**, 10713–10725 (1998).
60. Yienger, J. J. & Levy, H. Empirical model of global soil-biogenic NO_x emissions. *J. Geophys. Res.* **100**, 11447–11464 (1995).
61. Murray, L. T., Jacob, D. J., Logan, J. A., Hudman, R. C. & Koshak, W. J. Optimized regional and interannual variability of lightning in a global chemical transport model constrained by LIS/OTD satellite data. *J. Geophys. Res.* **117**, 20307 (2012).
62. Ott, L. E. et al. Production of lightning NO_x and its vertical distribution calculated from three-dimensional cloud-scale chemical transport model simulations. *J. Geophys. Res.* **115**, D04301 (2010).
63. Price, C. & Rind, D. Modeling global lightning distributions in a general circulation model. *Mon. Weather Rev.* **122**, 1930–1939 (1994).
64. Johnston, F. H. et al. Estimated global mortality attributable to smoke from landscape fires. *Environ. Health Perspect.* **120**, 695–701 (2012).
65. Burnett, R. T. et al. An integrated risk function for estimating the global burden of disease attributable to ambient fine particulate matter exposure. *Environ. Health Perspect.* **122**, 397–403 (2014).
66. Jiang, X. et al. Revealing the hidden health costs embodied in Chinese exports. *Environ. Sci. Technol.* **49**, 4381–4388 (2015).
67. Lelieveld, J. et al. Loss of life expectancy from air pollution compared to other risk factors: a worldwide perspective. *Cardiovasc. Res.* **116**, 1910–1917 (2020).
68. Dicker, D. et al. Global, regional, and national age-sex-specific mortality and life expectancy, 1950–2017: a systematic analysis for the Global Burden of Disease Study 2017. *Lancet* **392**, 1684–1735 (2018).
69. *Global Health Data Exchange* (Institute for Health Metrics and Evaluation, accessed 17 March 2021); http://ghdx.healthdata.org/gbd-results-tool
70. *Population Estimates and Projections* (World Bank Group, 2011); https://databank.worldbank.org/source/population-estimates-and-projections
71. CIESIN *Gridded Population of the World, Version 4 (GPWv4): Population Count Adjusted to Match 2015 Revision of UN WPP Country Totals, Revision 11* (NASA SEDAC, 2018).
72. Kc, S. & Lutz, W. The human core of the Shared Socioeconomic Pathways: population scenarios by age, sex and level of education for all countries to 2100. *Glob. Environ. Change* **42**, 181–192 (2017).
73. Hughes, B. B. et al. Projections of global health outcomes from 2005 to 2060 using the International Futures integrated forecasting model. *Bull. World Health Org.* **89**, 478–486 (2011).
74. Tong, D. et al. Dantong2021/Dantong2021-Globalpower_in_scenarios: global power emissions. *Zenono* https://doi.org/10.5281/zenodo.5637476 (2021).

Acknowledgements

This work was supported by the National Natural Science Foundation of China (grant nos. 41921005 and 41625020) and the Energy Foundation (G-2009-32416). D.T. was supported by a gift to Carnegie Institution for Science from Gates Ventures LLC. C.H. and S.J.D. were supported by the US National Science Foundation (Innovations at the Nexus of Food, Energy and Water Systems grant no. EAR 1639318).

Author contributions

Q.Z., D.T. and S.J.D. designed the study. D.T. performed the emission and health analyses with support from J.C., X.Q. and C.H. on analytical approaches. G.G. conducted GEOS-Chem simulations. D.T., S.J.D. and Q.Z. interpreted the data. D.T., S.J.D., G.G. and Q.Z. wrote the paper with input from all co-authors.

Competing interests

The authors declare no competing interests.

Additional information

Extended data is available for this paper at https://doi.org/10.1038/s41558-021-01216-1.

Supplementary information The online version contains supplementary material available at https://doi.org/10.1038/s41558-021-01216-1.

Correspondence and requests for materials should be addressed to Qiang Zhang or Steven J. Davis.

Peer review information *Nature Climate Change* thanks Jan Steckel and the other, anonymous, reviewer(s) for their contribution to the peer review of this work.

Reprints and permissions information is available at www.nature.com/reprints.

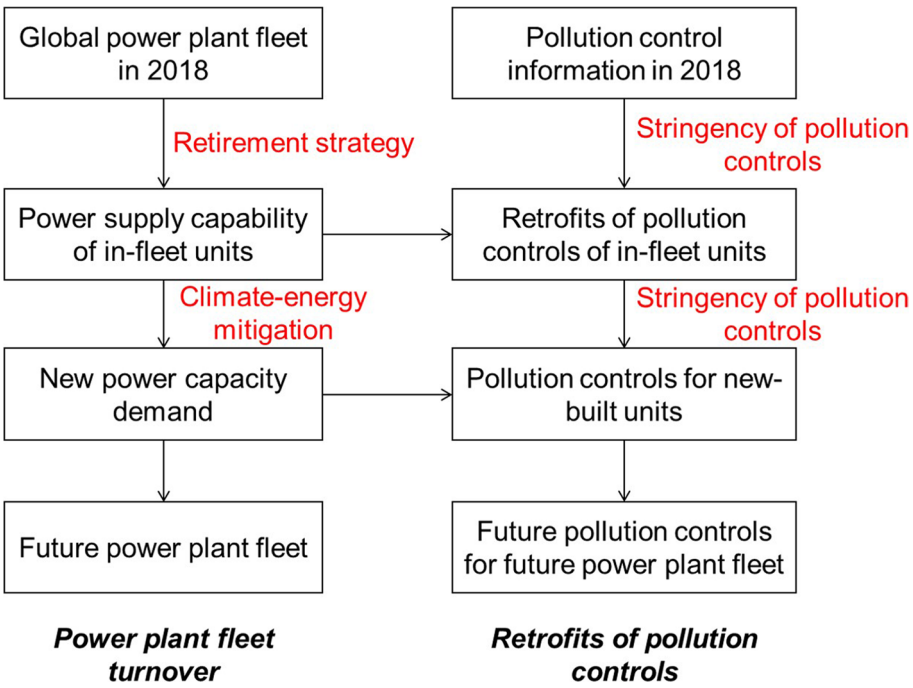

Extended Data Fig. 1 | The framework of unit-level power emission projection model. The figure shows the framework of unit-level power emission projection model developed for this study.

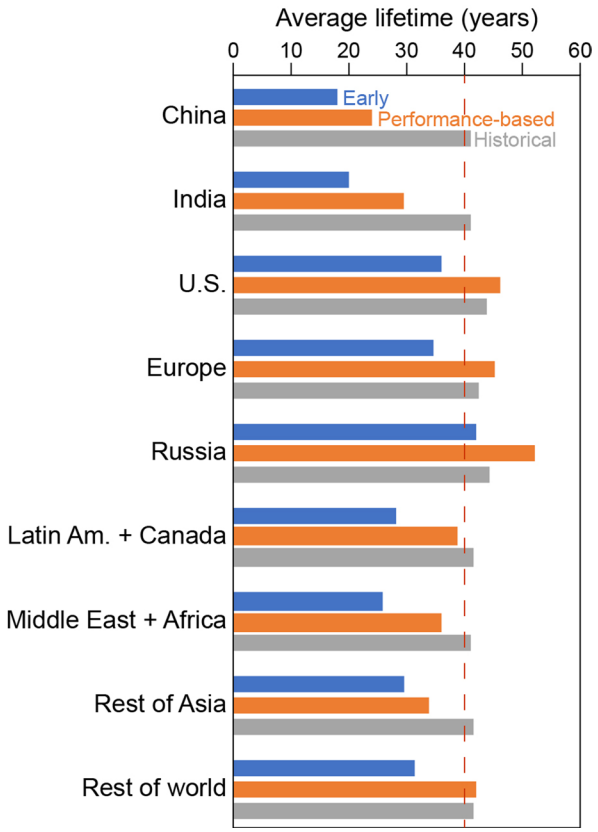

Extended Data Fig. 2 | Regional average lifetimes for each retirement strategy. The figure shows the regional average lifetimes of power plants for each retirement strategy.

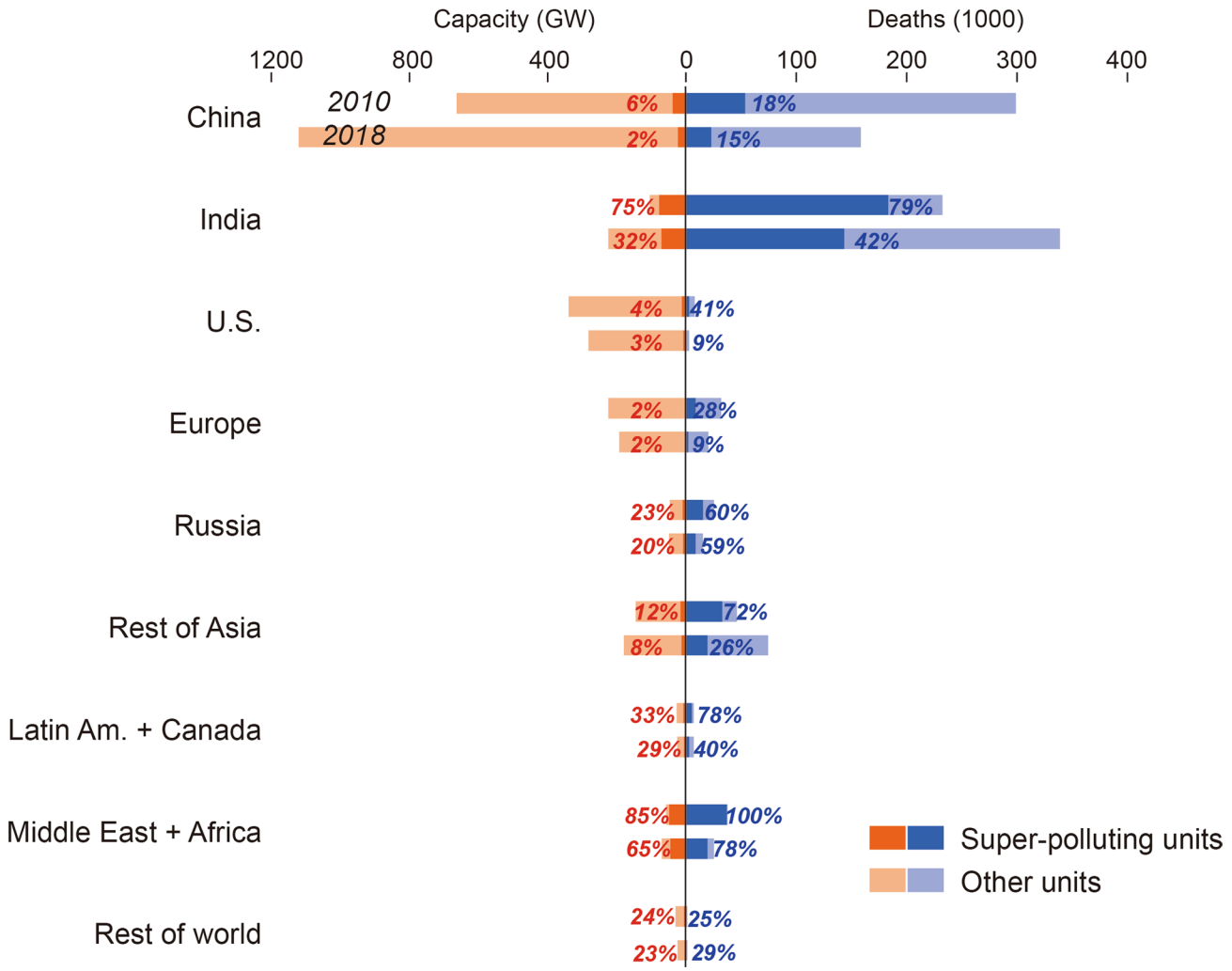

Extended Data Fig. 3 | Identified capacity and death contributions of 2010-coal super-polluting units. The figure shows capacity and death contributions of 2010-coal super-polluting units in 2010 and 2018 across nine regions.

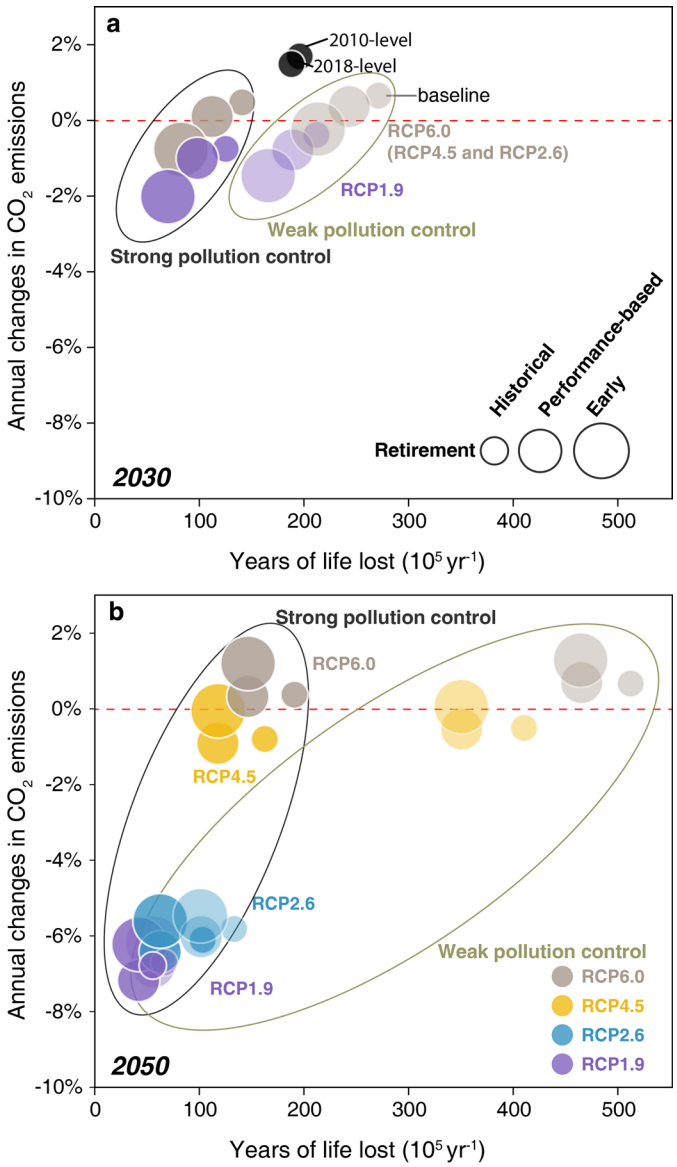

Extended Data Fig. 4 | Mean annual change in CO_2 emissions and $PM_{2.5}$-related years of life lost. The figure shows the relationship between annual average CO_2 reduction rate and $PM_{2.5}$-related years of life lost under the scenario assemble in **(a)** 2030 and **(b)** 2050, spanning four levels of climate ambition (RCP6.0, RCP4.5, RCP2.6, and RCP1.9) and three different retirement strategies (historical, performance-based, and early retirement) and two stringencies of pollution controls (that is strong and weak). The black circles show the mean annual change in CO_2 emissions during 2010–2015 (and 2010-level $PM_{2.5}$-related years of life lost), and 2010–2018 (and 2018-level $PM_{2.5}$-related years of life lost), respectively.

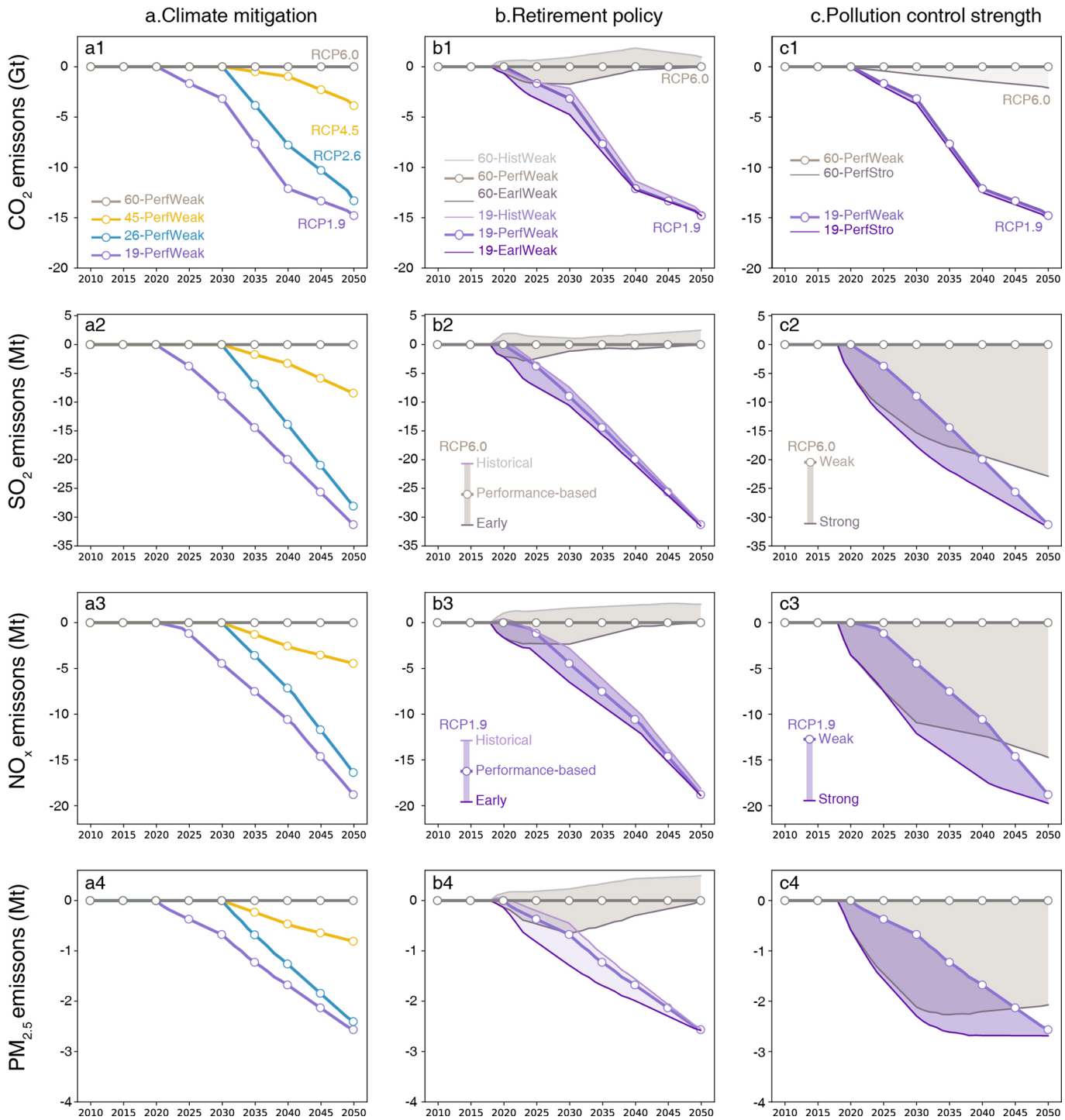

Extended Data Fig. 5 | Future emission reductions during 2010–2050 under various combined mitigation options. The period during 2010–2018 show the real emission differences, equalling 0. The RCP6.0 with performance-based retirement and weak pollution control scenario was set as the base scenario for comparison, Figs. a1-a4 show the emission reductions among different ambitious climate-energy scenarios (that is RCP4.5, RCP2.6, and RCP1.9); Figs. b1-b4 show the emission changes among different retirement strategies (that is historical and early retirements) covering RCP6.0 and RCP1.9; Figs. c1-c4 show the emission reductions from weak to strong pollution controls covering RCP6.0 and RCP1.9.